

OPAL Conference Report CR460  
November 5, 2018  
hep-ex/0101015

# Searches at LEP

Tom Junk

*Carleton University*  
*1125 Colonel By Drive, Ottawa, Canada K1S 5B6*

## Abstract

Searches have been conducted for a broad range of new phenomena by the four experiments ALEPH, DELPHI, L3, and OPAL, at LEP2. Each experiment contributes approximately  $150 \text{ pb}^{-1}$  of  $e^+e^-$  annihilation data with a mean  $\sqrt{s}$  of 205.9 GeV in 2000 to these searches (data prepared for the September 5 LEPC meeting). The statistical procedure for setting limits and evaluating the significance of excesses observed in the data is reviewed. Search results are presented for the Standard Model Higgs boson, the neutral Higgs bosons in the MSSM, charged Higgs bosons, invisibly decaying Higgs bosons produced by Higgs-strahlung, and fermiophobic Higgs bosons. Search results are briefly summarized for gauginos, stops, and staus. The photon recoil spectrum is checked for hints of new physics.

Results presented here have been prepared by the four LEP Collaborations, ALEPH, DELPHI, L3, and OPAL, and by the LEP Higgs and SUSY working groups, for presentation at the September 5 open meeting of the LEP experiments committee (LEPC).

Presented at the 5<sup>th</sup> International Symposium on  
Radiative Corrections  
Carmel, California, September 11–15, 2000

# 1 Introduction

In 1995, LEP finished taking large samples of data on the  $Z^0$  resonance and began a program of increasing the beam energy in order to study in detail known phenomena at higher energies and to search for new particles and interactions. The very highest beam energies were reached in 2000, and in that year each experiment collected  $\approx 150 \text{ pb}^{-1}$  of  $e^+e^-$  annihilation data at an average  $\sqrt{s}$  of approximately 205.9 GeV for inclusion in the results presented at the September 5, 2000 meeting of the LEP Experiments Committee (LEPC). In addition, the searches for the SM and MSSM Higgs bosons were combined by the LEP Higgs Working Group and shown at the LEPC meeting and are summarized here. The search for a neutral Higgs boson produced in association with a  $Z^0$  boson is emphasized here because of recent interest generated by excess events observed by the ALEPH collaboration in the summer of 2000. In addition, a brief selection of searches for supersymmetric particles is given, and a summary of the running strategy for the rest of 2000 is presented.

The main Standard Model backgrounds for the searches described here are

- Two-photon processes,  $e^+e^- \rightarrow e^+e^-\bar{f}f$ , where the  $\bar{f}f$  pair has a very low invariant mass and is produced in  $t$ -channel exchange of two photons.
- Radiative returns to the  $Z^0$ . Initial state radiation (ISR) reduces the effective  $\sqrt{s}$  to the  $Z^0$  pole energy and produces boosted  $Z^0$  events. The photon usually escapes down the beampipe, but may be observed, and the probability of two hard photons increases with increasing  $\sqrt{s}$ . These events are backgrounds to analyses requiring missing energy, and electromagnetic coverage is needed very close to the beam axis in order to suppress this background to searches requiring missing transverse momentum.
- W-pair production  $e^+e^- \rightarrow W^+W^-$ . These produce four-jet final states, or jets+a lepton+missing energy, or two leptons and missing energy. The last is classified as an “acoplanar dilepton” because the plane containing the two leptons does not in general contain the beam axis. Very few b quarks are produced in W decay and so this background can be suppressed in Higgs searches with b-tags with good background rejection. Searches for acoplanar dileptons have  $W^+W^-$  production as an

irreducible background in some kinematic regions, while the two-photon background dominates in other regions.

- Z-pair production,  $e^+e^- \rightarrow Z^0Z^0$ . These events may have four jets, two jets and missing energy, two jets and two like-flavor but opposite-sign leptons, four leptons, or two leptons and missing energy. They have a high b quark content and constitute a primary irreducible background to Higgs boson searches.
- Single W production,  $e^+e^- \rightarrow W^+e^-\bar{\nu}_e$ . This can produce jets+missing energy (“acoplanar dijets”), jets+a forward electron, or a lepton+missing energy or a lepton+a forward electron+missing energy.
- Single Z production  $e^+e^- \rightarrow Z^0e^+e^-$ . This process can produce acoplanar dijets or acoplanar dileptons if the electrons are not detected. One or both of the electrons may be detected however.

## 2 Statistical Procedure

A single procedure is used by the four experiments and by the LEP Higgs and SUSY working groups to determine whether a model of new physics is excluded by LEP search data or if the background hypothesis is disfavored relative to a particular signal hypothesis. The procedure begins with a full specification of the model to test, with the masses, production cross-sections, and decay branching ratios specified. If the model under test allows many possibilities for the parameters, then in general the parameters are scanned and excluded regions are given in the parameter space that is allowed. For a specific model with a specific choice of its free parameters, histograms of the expected signal, background, and data events are formed in variables that separate the expected signal from the expected background. Then all possible experimental outcomes are considered, and they are ordered according to those that are more signal-like (more candidate events in bins where a signal is expected), and those that are more background-like (fewer such candidates). The variable used for ordering the outcomes is the “likelihood ratio,” the ratio of the probability of observing the particular outcome in the signal+background hypothesis to the probability of observing the same

outcome in the background-only hypothesis:

$$Q = \frac{P_{poiss}(data|signal + background)}{P_{poiss}(data|background)}. \quad (1)$$

Each bin of each histogram may be considered as an independent counting experiment, and the Poisson probabilities multiply. The expression for  $\log Q$  is convenient for combinations of many bins in many experiments:

$$\log Q = \sum_i \left( n_i^{data} \log \left( 1 + \frac{s_i}{b_i} \right) - s_i \right), \quad (2)$$

where  $s_i$  is the signal estimation for a bin of a search channel,  $b_i$  is the background estimation,  $n_i^{data}$  is the number of observed data events, and the sum runs over all bins in all search channels. Some searches may have just one bin in them, while others may have some regions of histograms of measured variables with good separation of the signal from the background and other regions with poorer separation. Because  $\log Q$  reduces to a sum of event weights, events may be classified by the  $s/b$  in the bins in which they appear.

A particular value of  $\log Q$  will be obtained for each model hypothesis and the available data and background estimates. In order to determine whether an outcome is sufficient to exclude that model, the probability of obtaining that outcome in the signal+background hypothesis is computed:

$$CL_{s+b} = P(Q \leq Q_{obs}|signal + background). \quad (3)$$

If  $CL_{s+b} < 0.05$  then the signal+background hypothesis is ruled out at the 95% confidence level. Another important confidence level to compute is the consistency of the observation with the background hypothesis:

$$CL_b = P(Q \leq Q_{obs}|background), \quad (4)$$

which is the probability of having observed no more than was observed, if only background processes contribute. This variable is used as the “discovery” variable, requiring  $1 - CL_b < 5.7 \times 10^{-7}$  in order to claim a  $5\sigma$  discovery. These confidence levels may be computed using Monte Carlo techniques [1], or by various convolution methods [2], [3].

One defect of the  $CL_{s+b}$  variable is that it is a test of the signal+background hypothesis and not of just the signal hypothesis. A consequence of this is that

a deficit of selected events relative to the background estimation can rule out the background hypothesis alone, and therefore also any signal+background hypothesis, even if the signal is vanishingly small. In fact, this is expected to happen 5% of the time at the 95% confidence level. In order not to produce misleading limits or exclusions of parts of parameter space to which the experiments are not sensitive, the following quantity is used [1]:

$$CL_s = CL_{s+b}/CL_b, \quad (5)$$

which is expected to approach unity in the absence of sensitivity to a particular signal.

### 3 Standard Model Higgs Boson Searches

The Standard Model Higgs boson is expected to be produced in  $e^+e^-$  collisions mainly by the Higgs-strahlung process when it is kinematically allowed, and to a lesser extent by the  $W^+W^-$ -fusion process. The main attraction of the latter process is that its cross-section does not drop rapidly near  $\sqrt{s} - m_Z$ , although its total rate is very small. The total production cross-section near the kinematic edge is of the order of 50 to 500 fb, depending on how close  $m_H$  is to  $\sqrt{s} - m_Z$ . The Standard Model Higgs boson is expected to decay predominantly into  $b\bar{b}$  pairs in the mass range of interest, with a branching ratio of 78% at  $m_H=110$  GeV and a branching ratio of 74% at  $m_H=115$  GeV. The second most important decay mode is to tau pairs, with a branching ratio of approximately 7%, and the  $W^+W^-$  decays take 8%, which rises quickly with  $m_H$ . Decays to charm and gluons account for the remainder. Efficient and pure b-tagging is therefore important for search for Higgs bosons at LEP2. The Standard Model Higgs search channels are differentiated by the  $Z^0$  decay mode that they select. There is the four-jet channel ( $H^0 \rightarrow b\bar{b}, Z^0 \rightarrow q\bar{q}$ ), the missing-energy channel ( $H^0 \rightarrow b\bar{b}, Z^0 \rightarrow \nu\bar{\nu}$ ), the tau channels ( $H^0 \rightarrow b\bar{b}, Z^0 \rightarrow \tau^+\tau^-$  and  $H^0 \rightarrow \tau^+\tau^-, Z^0 \rightarrow q\bar{q}$ ), and the lepton channels ( $H^0 \rightarrow b\bar{b}, Z^0 \rightarrow e^+e^-$  or  $Z^0 \rightarrow \mu^+\mu^-$ ).

Precision electroweak measurements may be used to estimate the value of the Higgs boson mass, assuming the Standard Model framework for radiative corrections. The combined prediction of  $m_H$  is  $62_{-39}^{+53}$  GeV, where the errors are symmetric and Gaussian in the variable  $\log m_H$ , as reported at ICHEP 2000 [4]. This prediction changes, however, when  $\alpha_{EM}(m_Z)$  is computed

differently or computed using additional low-energy  $e^+e^- \rightarrow q\bar{q}$  cross-section data from BES.

In the absence of new particles and interactions, the mass of the Standard Model Higgs boson can be from approximately 140 GeV to 180 GeV, where the lower bound arises from a vacuum stability argument, and the upper bound from the requirement that the Higgs self-coupling remains finite at all energies. For new physics interactions with a scale of the order of a TeV, the Higgs boson mass is much less constrained by these arguments, lying between 50 to 800 GeV [5]. Fine tuning arguments [6], requiring that the magnitude of the radiative corrections to  $m_H$  are not too many orders of magnitude larger than  $m_H$  itself, further restrict the possible ranges of  $m_H$  although these restrictions are relaxed if new physics appears on the 1–10 TeV scale.

The combined distribution of the reconstructed masses in the four experiments' Standard Model Higgs boson searches is shown in Figure 1 for a fairly tight set of selection requirements [7]. Along with the background expectation and the observed data counts is shown the expected signal from a Higgs boson of mass 114 GeV. The contributions to the histogram are given by experiment in Table 1.

The distribution of the reconstructed mass and the the total number of selected events may be uninformative or misleading in several ways. The distribution of the reconstructed mass is summed over different experiments, and over different search channels at different center-of-mass energies. The reconstructed mass resolutions are different and depend on how close  $m_H$  is to the kinematic limit which changes with  $\sqrt{s}$ , and the relative amounts of the signal and background are different from channel to channel, depending on the background rates and signal branching ratios. In a summed histogram of the reconstructed mass, candidates in relatively clean channels are included in the same bins as signal and background estimates from other channels with poorer performance. Additional cuts have been applied after the standard analysis cuts in order that the contributions from the different experiments are roughly equal in their total size. If an experiment has a large amount of the expected signal just failing the cut needed to make the reconstructed mass distribution plot, it may be more sensitive than another experiment with more expected signal on its side of its cut. Because all bins of all histograms in all variables (each search channel from each experiment at each center of mass energy has its own histogram, and the variables can be the reconstructed mass, the b-tags, or combinations of these and other

information) can be combined using the uniform procedure outlined above, there is no loss of sensitivity in the confidence level calculations, but an amount of information is necessarily lost when producing a histogram of the reconstructed mass and tables listing its contents.

The full amount of information in the searches is retained and displayed in a compact form if the histograms are rebinned in the variable  $s/b$ . For each bin of each histogram to be combined, the  $s/b$  is uniquely determined. Because the test-statistic  $\log Q$  is additive and depends only on the  $s/b$  in the bins where the candidates are found and also on the total signal sum, the contents of bins with the same  $s/b$  may be simply added. The result is shown in Figure 2 along with its integral from the high  $s/b$  side [7]. The integral of this distribution at a particular cut in  $s/b$  is the optimal answer to “How many events are observed” and “How many are expected in the signal+background and the background-only hypotheses,” for each possible setting of the cuts.

One observes in this distribution three events with rather high values of the local  $s/b$ . These three are all four-jet candidates from ALEPH, with strong b-tags and high reconstructed masses [8]. The selection of these events and the stability of their assigned significance has been checked in several ways. A cut-based analysis is used to cross-check the primary neural-net-based analysis and similar results are obtained. All lower-energy data have been analyzed to look for biases in the reconstructed mass distribution towards a peak at the maximum kinematically allowed value, and no such bias is seen. The b-tag and neural net distributions also are modeled well [8]. One feature however, is that if all possible jet pairings are considered and events are removed if even one of these pairings yields jet-pair masses within 10 GeV of either  $m_W$  or  $m_Z$ , then the excess vanishes. It was found in a Monte Carlo study, however, that the signal efficiency drops by 50% by removing such events, and that this procedure does not enhance the separation of signal from background.

There is a small excess observed in the DELPHI four-jet channel, but not in the L3 or OPAL four-jet channels. Also, no excesses are observed in the combined missing-energy ( $Z^0 \rightarrow \nu\bar{\nu}$ ) channels, the lepton channels, or the tau channels. Combining all missing-energy, lepton, and tau channels together has about the same statistical power of all four-jet channels combined together.

The combined test-statistic is shown in Figure 3. It has a minimum at  $m_H=114-115$  GeV, and is the most compatible with the median expected

signal at  $m_H=114$  GeV. The confidence levels are used to quantify how significant this observation is.

The exclusion limit is computed by finding the lowest  $m_H$  for which  $CL_s = 0.05$ . It is computed for each experiment separately, and for each search channel separately, combining the results of the experiments. The expected limit is the median in a large ensemble of possible experiments in which only Standard Model background processes contribute. The value of  $CL_s$  and its expectation for the all channels combined from all experiments is shown in Figure 4. The exclusion limits are listed in Table 2. The branching ratios of the  $Z^0$  are well known and hence the separation by channel is not that interesting, except for the tau channel, which covers also Higgs boson decays to tau leptons.

In order to test for the compatibility of the observation with the expected background,  $1 - CL_b$  is shown as a function of the tested  $m_H$  in Figure 5.  $1 - CL_b$  reaches its minimum at  $m_H=115$  GeV, with a probability of consistency of the data with the background of  $7 \times 10^{-3}$ , for a significance of approximately  $2.6\sigma$ , due mainly to the excess four-jet events in ALEPH, but also to events with lower values of  $s/b$  which also contribute.

In the case that there is no signal truly present, the excess would take approximately  $60 \text{ pb}^{-1}$  per experiment at  $\sqrt{s} = 206.6$  GeV to fade away to a  $2\sigma$  excess for test mass hypotheses near 115 GeV. On the other hand, if the Higgs boson does have Standard Model couplings and branching fractions, then one would expect the significance of the excess to increase as more data are collected. As can be seen in Figure 6, it would take approximately  $100 \text{ pb}^{-1}$  of data at  $\sqrt{s} = 206.6$  GeV to obtain a  $4\sigma$  effect for  $m_H=113$  GeV, and around  $140 \text{ pb}^{-1}$  for  $m_H=114$  GeV. On the other hand, significances of  $3\sigma$  can be obtained within  $60 \text{ pb}^{-1}$  for  $m_H$  all the way up to 115 GeV, and that amount can be collected in approximately 60 days of running.

## 4 Searches for Non-Standard Higgs Bosons

### 4.1 Neutral Higgs Bosons in the MSSM

One of the simplest extensions to the Higgs sector of the Standard Model is to add a second Higgs field doublet. The Minimal Supersymmetric Extension of the SM (MSSM) requires this structure. One field couples to up-type quarks and the other to down-type quarks, and there is a mixing angle  $\alpha$



between these two fields in order to produce the physical Higgs states, which number five: the  $h^0$ , the  $A^0$ , the  $H^0$ , and two charged Higgs bosons  $H^+$  and  $H^-$ . The ratio of the vacuum expectation values of the two fields is denoted  $\tan\beta$ . In the CP-conserving, low-energy effective MSSM studied here [9], the remaining parameters are the mass of the  $A^0$ , the CP-odd Higgs boson (the other two neutral bosons are CP even), the mass scale of the sfermions  $M_{\text{SUSY}}$  (here set to 1 TeV), the Higgs mass matrix parameter  $\mu$  (here set to -200 GeV), the gaugino mass parameter  $M_2$  (here set to 200 GeV), and the amount of stop mixing, chosen here to be zero or maximal. Recent calculations of  $m_h$  including the dominant 2-loop terms are used [10]. The gluino mass is also a free parameter; it affects the Higgs masses and branching ratios through radiative corrections.

For the case of maximal stop mixing, and the choices of the other parameters given above, the value of  $m_h$  assumes its maximal value<sup>1</sup> as a function of  $\tan\beta$  and is used to set conservative limits on  $\tan\beta$ . This scenario is called the  $m_h$ -max scenario.

The searches used to set limits in this space are the same searches for the  $h^0Z^0$  final state used in the Standard Model section, but in addition, searches for  $h^0A^0$  are performed in the  $b\bar{b}b\bar{b}$  and  $b\bar{b}\tau^+\tau^-$  final states. The production cross-section for  $e^+e^- \rightarrow h^0A^0$  is proportional to  $\cos^2(\beta - \alpha)$ , which is largest for  $m_h \approx m_A$  while the cross-section for  $e^+e^- \rightarrow h^0Z^0$  is proportional to  $\sin^2(\beta - \alpha)$ . The cross-section for  $h^0A^0$  production grows more slowly along the diagonal  $m_h = m_A$  than the  $h^0Z^0$  cross-section does for large  $m_A$ . Therefore, the absolute lower limits on  $m_h$  will come from the case in which  $h^0Z^0$  production is suppressed, and the limits for  $m_A \rightarrow \infty$  are those obtained in the Standard Model, as can be seen from Figure 7.

For the case of no stop mixing, the maximal value of  $m_h$  as a function of  $\tan\beta$  is much less, although a second problem opens up at low  $\tan\beta$ : the branching ratio for  $h^0 \rightarrow b\bar{b}$  can be suppressed by a larger decay width for  $h^0 \rightarrow A^0A^0$ , and for low  $\tan\beta$  or low  $m_A$ , the decay rate of the  $A^0$  to  $b\bar{b}$  pairs is suppressed either by the coupling strength or the kinematics if  $m_A < 10$  GeV. In this case, an "L"-shaped unexcluded region opens up for low  $\tan\beta$  and low  $m_A$ , shown in Figure 8. Additional flavor-independent searches, and searches specifically targeted at this region are being developed and will

---

<sup>1</sup>Another calculation [11] using a renormalization-group improved one-loop calculation, does in fact give slightly higher values of  $m_h$  for  $\tan\beta < 1$ , but also smaller values of  $m_h$  for  $\tan\beta > 1$  – we choose the calculation which gives the lowest upper end of the excluded  $\tan\beta$  region.

soon be included in the combination. The limits on  $m_h$  and  $m_A$  presented in Table 3 ignore this unexcluded region, although the limits on  $\tan\beta$  in the no-stop-mixing scenario include its effects. In both the  $m_h$ -max scenario and the no stop mixing scenario,  $\tan\beta$  is considered only up to 30, because for larger values of  $\tan\beta$  the  $h^0$  decay width can exceed the experimental mass resolution, and additional Monte Carlo signal samples are needed to assess the effect of lower  $s/b$  in these channels.

A third scenario has been proposed, called the “large- $\mu$ ” scenario [9], in which  $M_{\text{SUSY}}$  is taken to be 400 GeV,  $M_2 = 400$  GeV,  $\mu = 1$  TeV, and the gluino mass is 200 GeV. This setting of parameters is designed to highlight loop effects which can suppress the decay  $h^0 \rightarrow b\bar{b}$ , without a corresponding enhancement of  $h^0 \rightarrow \tau^+\tau^-$ . In this case, the  $h^0$  decays rather into gluons, charmed quarks, or W pairs, but only for high  $\tan\beta$ . The decay widths of the  $h^0$  and the  $A^0$  remain much smaller than the experimental mass resolution up to  $\tan\beta = 50$ . The maximum value of  $m_h$  in this scenario is approximately 108 GeV, and for the region where  $\sin^2(\beta - \alpha)$  is low and  $m_h + m_A$  is kinematically out of reach at LEP2, the process  $e^+e^- \rightarrow H^0 Z^0$  is accessible with a cross-section proportional to  $\cos^2(\beta - \alpha)$ . Nearly all model points except those with difficult decay branching fractions can therefore be excluded. These difficult regions are at  $\tan\beta > 10$  and  $80 < m_A < 180$ , as seen in Figure 9.

## 4.2 Charged Higgs Bosons

At LEP, charged Higgs bosons are expected to be pair-produced via the  $s$ -channel exchange of a  $\gamma$  or a  $Z^0$ , and the production cross-section depends only on the mass of the  $H^\pm$  and on well-measured electroweak parameters. The decay modes of the  $H^\pm$  are considered for the purpose of these searches to be limited to  $q\bar{q}'$  and  $\tau\nu_\tau$ . The mass limits are produced therefore as a function of  $\text{Br}(H^+ \rightarrow \tau^+\nu_\tau)$ . The search channels include a four-jet search without b-tagging, a semileptonic search, and a fully leptonic search, in which the final state consists of an acoplanar pair of taus. The predominant background is  $e^+e^- \rightarrow W^+W^-$ , which can produce all of the available final states, although the acoplanar tau pair rate is significantly lower than the four-jet rate due to the branching ratios of the W. The large  $W^+W^-$  background sets the scale for the limits in the hadronic and semileptonic searches. The limits are shown in Figure 10. For  $\text{Br}(H^+ \rightarrow \tau^+\nu_\tau)=0$ , the observed mass limit is 80.5 GeV and the median expected limit is 79.8 GeV. For  $\text{Br}(H^+ \rightarrow \tau^+\nu_\tau)=1$ , the ob-

served mass limit is 89.2 GeV and the median expected limit is 90.9 GeV. The lowest limit obtained at any branching ratio is 78.7 GeV, with a median expectation of 78.5 GeV. A small excluded “island” appears in Figure 10 for  $\text{Br}(H^+ \rightarrow \tau^+ \nu_\tau) = 0$ , where the search sensitivity above the  $W^+W^-$  background peak is beginning to become sufficient to exclude a small region. More data would allow this island to grow and eventually connect with the main excluded region, leaving a hole near  $m_W$  which can be excluded only with a larger amount of integrated luminosity.

### 4.3 Searches for $H^0 \rightarrow \gamma\gamma$

The final states  $q\bar{q}\gamma\gamma$ ,  $\ell^+\ell^-\gamma\gamma$ , and  $\gamma\gamma$ +missing energy are sought by the four LEP experiments and combined. Because the branching ratio  $\text{Br}(H^0 \rightarrow \gamma\gamma)$  is small in the Standard Model (of the order  $10^{-3}$ ), mass limits cannot be set on the SM Higgs from this search only. This search is more interesting when considering models in which the  $H^0$  decays are non-standard. In particular, if the  $H^0$  fails to couple to fermions entirely, then the available decay modes are into  $\gamma\gamma$  and  $W^+W^-$ , the first of which proceeds only at the one-loop level mediated by a  $W$  boson. As the mass of the  $H^0$  increases, the  $W^+W^-$  branching fraction gradually becomes more important and the mass limits obtained at LEP2 are mainly determined by this behavior than by the power of the searches. The limits are expressed in Figure 11 by assuming the SM production cross-section for  $e^+e^- \rightarrow H^0 Z^0$ , and by ignoring the results of searches for other decays of the  $H^0$  to set limits on the branching ratio  $\text{Br}(H^0 \rightarrow \gamma\gamma)$ . Alternatively, this can be interpreted as a limit on the production cross-section as a fraction of the SM cross-section, with  $\text{Br}(H^0 \rightarrow \gamma\gamma) = 1$ . In the fermiophobic model, the observed mass limit is 107.7 GeV, with a median expected limit of 105.8 GeV.

### 4.4 $h^0 \rightarrow$ Invisible Particles

The Higgs boson may decay invisibly in the MSSM if the lightest neutralino has a mass of less than half the mass of the Higgs. Two important advantages of an  $e^+e^-$  collider are that the center-of-mass energy of each interaction is known with a high degree of precision, and that the total momentum is zero. These features can be used to search for the process  $e^+e^- \rightarrow h^0 Z^0$ , where the  $h^0$  decays invisibly, because the  $Z^0$  decay products can be measured and the missing mass can be inferred. In this case,  $Z^0$  decays to quarks are exploited

for the search. Neutrino decays are not useful, and the leptonic decays have a low relative branching ratio. Tau decays in particular pollute the leptonic sample because the neutrinos in such events carry a large amount of missing energy.

The limits are shown in Figure 12 assuming the Standard Model production cross-section and are limits on the invisible branching ratio of the Higgs, ignoring the results of searches for visible Higgs decays. Alternatively, these limits can be interpreted as limits on the production cross-section divided by the Standard Model production cross-section, assuming 100% invisible decays of the  $h^0$ . For the SM cross-section and 100% invisible decays, the mass limits obtained are 113.7 GeV (observed) and 112.8 GeV (median expectation).

## 5 Gaugino, Squark, Slepton Searches

Charginos may be produced either in the  $s$ -channel via photon or  $Z^0$  exchange, or in the  $t$ -channel via exchange of an electron sneutrino. These diagrams interfere destructively, although the  $t$ -channel diagram is important only for light electron sneutrinos. The chargino may decay into a  $W$  and a neutralino, or into a slepton and a neutrino, where the slepton decays into a neutralino and a lepton, or directly into a lepton and a sneutrino. All of these decay modes produce similar final states – two leptons (or jets) and missing energy. The branching ratios for these processes depend on the slepton and sneutrino masses, and the mass difference  $\Delta M$  between the chargino and the LSP (either the neutralino or sneutrino) strongly affects the final state kinematic distributions. For a small mass difference, the visible decay products of the chargino have low visible energies. These final states are similar to the two-photon background processes which have large cross-sections in  $e^+e^-$  collisions at high energies. For very large  $\Delta M$ , the final states resemble  $W^+W^-$  production. The search analyses are therefore optimized in separate regions of  $\Delta M$  due to the different makeup of the signal and background estimations.

An important feature of the chargino searches is that the limits obtained approach the maximum possible kinematic limits rapidly due to the high expected production cross-sections, and so the extra data taken at  $\sqrt{s} \geq 208$  GeV is very useful in these searches. OPAL presents limits on the chargino production cross section in Figure 13. No evidence for a signal

is observed, although for the search with  $\Delta M \approx 10$  GeV, there is an excess observed [12] in the OPAL experiment: five events are counted in the data, while 0.74 events are expected from the sum of all Standard Model backgrounds. None of the other experiments sees a similar excess, and the significance is diluted by the fact that many different search regions in four experiments were independently investigated and that a fluctuation can happen in any of them.

Neutralinos may also be produced via  $s$ -channel  $Z^0$  exchange, or via  $t$ -channel selectron exchange, and the lightest neutralino  $\tilde{\chi}_1^0$  is assumed to be the lightest supersymmetric particle (LSP). Pair production of  $\tilde{\chi}_1^0\tilde{\chi}_1^0$  is impossible to detect aside from the signature of the residual initial state radiation. Instead, associated production of  $\tilde{\chi}_2^0\tilde{\chi}_1^0$  is sought, where  $\tilde{\chi}_2^0 \rightarrow \tilde{\chi}_1^0 Z^0$ , and the  $Z^0$  decay products are observed. The observable final states are then two jets and missing energy, or two leptons and missing energy, with similar backgrounds to the chargino searches. OPAL's limits on the neutralino production cross-section are shown in Figure 13.

Searches for sleptons similarly focus on the final state of two like-flavored, opposite-signed leptons with missing energy, produced by the process  $e^+e^- \rightarrow \tilde{\ell}^+\tilde{\ell}^-$  followed by  $\tilde{\ell}^+ \rightarrow \tilde{\chi}_1^0\ell^+$ . In the 1999 data, there was an excess of events passing the requirements of the stau searches in all four detectors – no single experiment had a significant effect, but in combination the significance was greater:  $1 - \text{CL}_b = 0.001$  when 1998 and 1999 data were combined [13], with a stau mass hypothesis of 85 GeV and a neutralino mass hypothesis of 22 GeV. However, the excess did not persist in the 2000 data collected by the four experiments, and the particular hypothesis mentioned above is now excluded at the 95% CL [14].

After the July 20 LEPC presentation by ALEPH reporting an excess in a preliminary search [15] for a very light sbottom (of mass between 3 and 4 GeV), the DELPHI and OPAL collaborations performed similar searches. OPAL sees a deficit of events, with 15 events observed and 20.5 events expected from Standard Model background processes [16]. DELPHI similarly does not see an excess [17]. The ALEPH experiment updated the search with an improved Monte Carlo and a lepton identification algorithm which is more appropriate for identifying leptons inside dense jets and does not report a significant excess, with 24 events observed and 20 events expected from Standard Model backgrounds [8].

## 6 The Photon Recoil Spectrum

Events containing a single high-energy photon are valuable for searching for non-interacting new particles, such as LSP neutralinos (already mentioned), or  $\tilde{\chi}_2^0 \rightarrow \tilde{\chi}_1^0 \gamma$ . In Gauge-mediated SUSY-breaking models, the gravitino can be the LSP, and  $\tilde{\chi}_1^0 \rightarrow \tilde{G} \gamma$  is possible. An excited neutrino may decay radiatively. In general, any invisible process may also be accompanied by initial state radiation which may be detected, giving a sign for new physics. Unfortunately, no excess is observed in the recoil mass spectrum to single and multiple photons, as shown in Figure 14, which combines [14] the four LEP experiments' results for all data taken with  $\sqrt{s} \geq 130$  GeV.

## 7 Prospects for Further LEP Running

The hint of an excess in the Standard Model Higgs searches near with  $m_H=115$  GeV has generated a good deal of interest in extending the LEP run through 2001 with an energy upgrade.

Since the RADCOR2K conference, there have been two additional updates of the significance of the SM Higgs search results, at the LEPC presentations of October 10, 2000 [18] and on November 3, 2000 [19], with significances reported of  $2.5\sigma$  and  $2.9\sigma$ , respectively. Some variation is expected in both the signal and background cases due to statistical fluctuations – large jumps in the significance occur with the discrete arrival of candidates with large local values of  $s/b$ .

At the November 3 LEPC open session, the ALEPH, DELPHI, L3 and OPAL collaborations and the LEP Higgs Working Group jointly recommended running LEP in 2001. On the same day, the LEP Experiments Committee met in a closed session and was undecided on the recommendation, balancing the construction schedule, the cost, and the staffing of the LHC against the LEP run request. The research board also failed to make a recommendation, and on November 8, 2000, a press release was issued that LEP was closed, and on November 15, 2000 a committee of the CERN council was convened, which also failed to endorse the run extension request. Dismantling LEP began in early December, 2000.

## Acknowledgements

The LEP accelerator has performed outstandingly well due to the hard work of the members of the accelerator divisions at CERN. In particular, the RF performance has improved throughout the year, miniramps and the bending-field spreading technique were commissioned, and the accelerator had a high reliability and short turnaround times, all due to hard work and good organization. The author would like to thank the members of the four LEP collaborations, and the members of the LEP Higgs working group for the exemplary cooperation and openness in supplying search results for combination.

## References

- [1] A. L. Read, *Optimal Statistical Analysis of Search Results Based on the Likelihood Ratio and its Application to the Search for the MSM Higgs boson at 161 and 172 GeV*, DELPHI note 97-158 PHYS 737 (1997).
- [2] H. Hu and J. Nielsen, *Analytic Confidence Level Calculations using the Likelihood Ratio and Fourier Transform*, physics/9906010 (1999).
- [3] T. Junk, Nucl. Instrum. Meth. **A434**, 435 (1999).
- [4] B. Pietrzyk, presentation given at the 30<sup>th</sup> International Conference on High Energy Physics, July 27 - August 2, 2000, Osaka, Japan.
- [5] P. Igo-Kemenes, Eur. Phys. J. **C15**, 274 (2000).
- [6] C. Kolda and H. Murayama, hep-ph/0003170 (2000).
- [7] C. Tully, presentation given to the open session of the LEP Experiments Committee, September 5, 2000. Available at [http://lephiggs.web.cern.ch/LEPHIGGS/talks/tully\\_talk.pdf](http://lephiggs.web.cern.ch/LEPHIGGS/talks/tully_talk.pdf).
- [8] D. Schlatter, presentation given to the open session of the LEP Experiments Committee, 5 September 2000. Available at [http://alephwww.cern.ch/ALPUB/seminar/lepc\\_sep00/lepc\\_0509.pdf](http://alephwww.cern.ch/ALPUB/seminar/lepc_sep00/lepc_0509.pdf).
- [9] M. Carena, S. Heinemeyer, C.E.M. Wagner, and G. Weiglein, “Suggestions for Improved Benchmark Scenarios for Higgs Boson Searches at LEP2”, hep-ph/9912223 (1999).
- [10] S. Heinemeyer, W. Hollik and G. Weiglein, Phys. Rev. **D58** 091701 (1998);  
S. Heinemeyer, W. Hollik and G. Weiglein, Eur. Phys. J. **C9** 343 (1999).
- [11] M. Carena, M. Quirós and C.E.M. Wagner, Nucl. Phys. **B461** (1996) 407, hep-ph/9508343.
- [12] C. Rembser, OPAL Collaboration presentation given to the LEPC open session, 5 September, 2000. Available at [http://opal.web.cern.ch/Opal/talks/rembser\\_lepc00/main.ps.gz](http://opal.web.cern.ch/Opal/talks/rembser_lepc00/main.ps.gz)



- [13] A. Favara, presentation given at SUSY2K, CERN, June 26 – July 1, 2000.
- [14] S. Lees-Rosier, LEP SUSY Working Group presentation given to the LEPC open session, 5 September, 2000. Available at [http://l3www.cern.ch/conferences/ps/Rosier\\_LEPC\\_susyww.ps.gz](http://l3www.cern.ch/conferences/ps/Rosier_LEPC_susyww.ps.gz)
- [15] G. Taylor, ALEPH Collaboration presentation given at the LEPC open session, July 20, 2000. Available at <http://alephwww.cern.ch/ALPUB/seminar/lepcjul00/lepc.ps>.
- [16] K. Hoffman, presentation given at the 30<sup>th</sup> International Conference on High Energy Physics, July 27 - August 2, 2000, Osaka, Japan.
- [17] T. Camporesi, DELPHI Collaboration presentation given to the LEPC open session, September 5, 2000. Available at [http://delphiwww.cern.ch/~pubxx/delsec/talks/LEPCsep2000/tc\\_lepc.pdf](http://delphiwww.cern.ch/~pubxx/delsec/talks/LEPCsep2000/tc_lepc.pdf)
- [18] T. Junk, LEP Higgs Working Group presentation given at the LEP Fest, October 10, 2000. Available at [http://lephiggs.web.cern.ch/LEPHIGGS/talks/tom\\_lepfest.ps](http://lephiggs.web.cern.ch/LEPHIGGS/talks/tom_lepfest.ps).
- [19] P. Igo-Kemenes, LEP Higgs Working Group presentation given at the LEPC open session, November 3, 2000. Available at <http://lephiggs.web.cern.ch/LEPHIGGS/talks/index.html>.

Experiment	Data	Background	Signal
ALEPH	7	3.3	1.0
DELPHI	5	5.4	1.3
L3	4	4.0	0.3
OPAL	11	9.6	0.9
<b>LEP</b>	<b>27</b>	<b>22.2</b>	<b>3.6</b>

Table 1: Numbers of observed events and the expected event counts from a 114 GeV Higgs boson signal and the Standard Model background processes.

Experiment	Observed (GeV)	Expected (GeV)
ALEPH	109.1	112.5
DELPHI	110.5	110.9
L3	108.8	110.2
OPAL	109.5	111.7
Channel	Observed (GeV)	Expected (GeV)
Leptons	109.9	108.8
Neutrinos	112.1	110.7
Taus	105.4	104.2
Four Jets	109.0	113.5
<b>LEP</b>	<b>112.3</b>	<b>114.5</b>

Table 2: Limits on the mass of the Higgs boson, assuming the Standard Model production cross-section and branching fractions, by experiment, by channel, and combined. These have been computed with a uniform procedure and may vary by small amounts from the ones quoted by the individual experiments. In the lepton channel, there is a small unexcluded region below 100.7 GeV.

Scenario	$m_h$ limit obs (GeV)	$m_h$ limit exp (GeV)	$m_A$ limit obs (GeV)	$m_A$ limit exp (GeV)	$\tan \beta$ limit obs	$\tan \beta$ limit exp
$m_h$ -max	89.5	93.8	90.2	94.1	0.53–2.25	0.48–2.48
No stop mix	89.4	94.3	89.6	94.6	0.9–7.2	0.8–15

Table 3: Limits on  $m_h$ ,  $m_A$ , and  $\tan \beta$  in the  $m_h$ -max and no-mixing scenarios. The limits obtained by the combination of the four LEP experiments’ data are indicated with “obs,” while the median limits expected to be obtained in a large ensemble of background-only experiments are labeled “exp.”

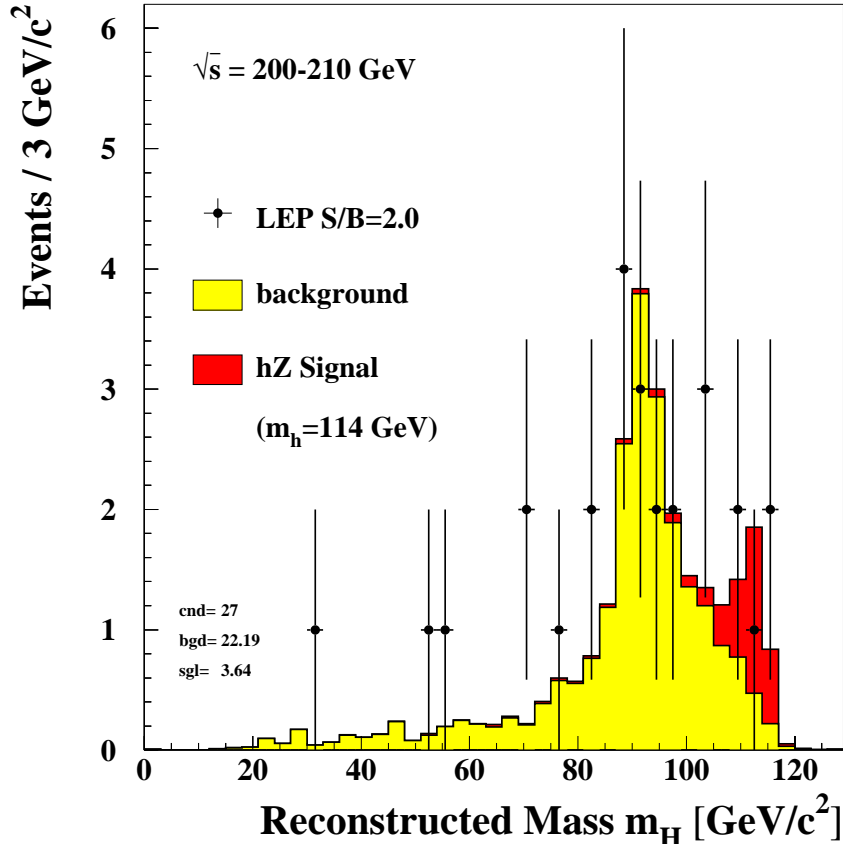


Figure 1: Distribution of the reconstructed masses of candidates selected by the Higgs search analyses summed over the four LEP experiments, summed over all search channels for the data taken in 2000. The selection cuts have been chosen such that the integrated signal divided by the integrated background for reconstructed masses above 109 GeV, for a SM signal hypothesis of 114 GeV, is roughly 2.0, in order to keep the contributions from the four experiments roughly similar. Each bin contains contributions from several sources with different s/b. The light histogram shows the sum of all SM background expectations, the dark histogram shows the expected signal from a 114 GeV Higgs boson, and the points show the data.

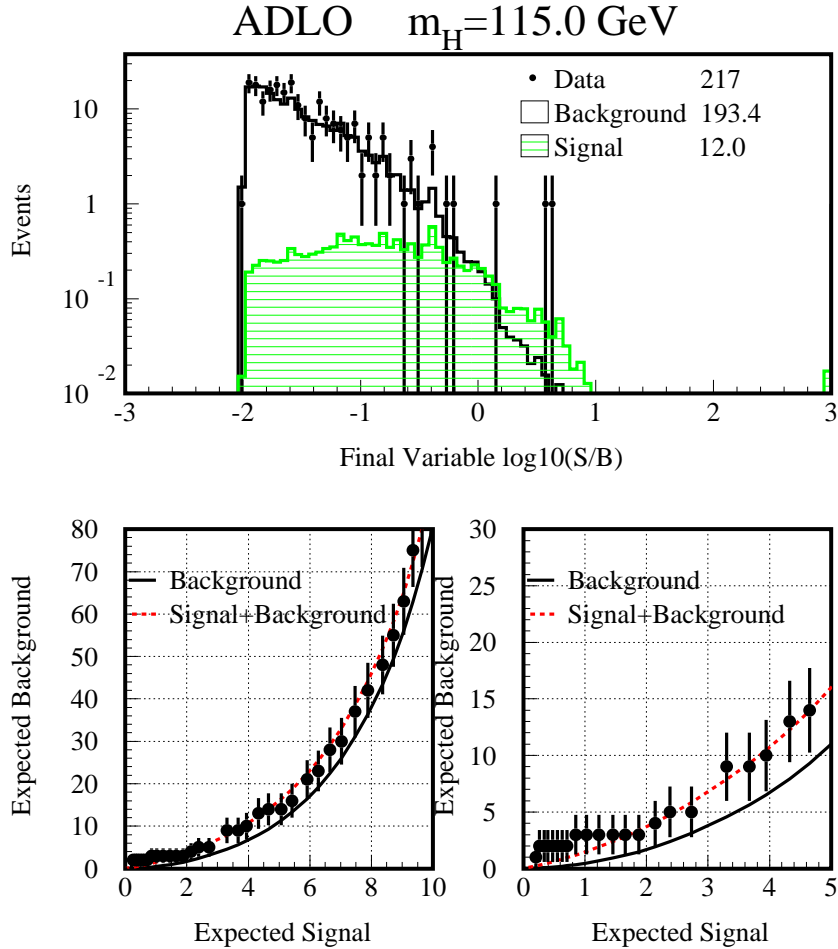


Figure 2: Distribution of the  $s/b$  for all bins of all search channels in all experiments at all energies. The signal is shown with a hatched histogram and the background with the open histogram. The data are shown with the points with error bars. The most significant candidates from the ALEPH experiment's four-jet channels are the three rightmost data points. The lower graphs show the integral of the  $s/b$  distribution shown in the upper panel, from the high  $s/b$  side. The background integral is the solid curve, the signal+background is the dashed curve, and the observed data are the points with error bars. Neighboring points are highly correlated because of the cumulative sum. The two lower panes show the same integrals, but on different horizontal scales.

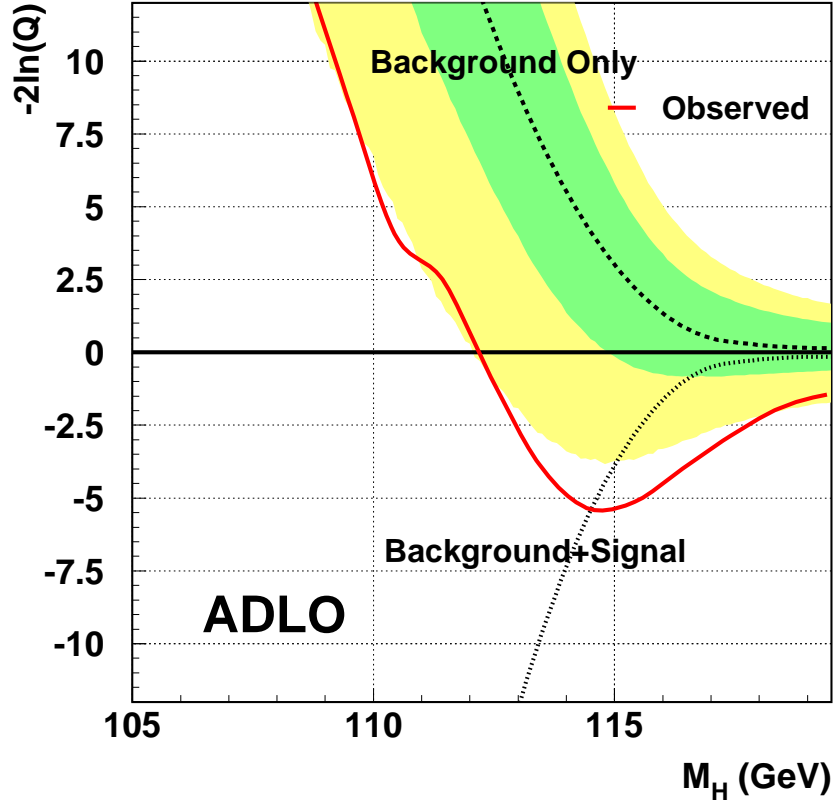


Figure 3: The value of the likelihood ratio test statistic  $-2\ln Q$  as a function of the test mass  $m_H$ . Values below zero indicate a preference of the data for the signal hypothesis. The solid curve shows the observation in the combined LEP data, the dashed curve shows the median expectation in an ensemble of background experiments, and the dotted curve shows the median expectation in an ensemble of experiments in which the background and a signal originating from a SM Higgs boson of mass equal to the test mass. The dark band around the median background expectation is the 68% probability interval for the background ensemble, centered on the median expectation, and the light bands indicate the 95% interval. The minimum of the observed  $-2\ln Q$  curve is at  $m_H=115$  GeV and has a value below zero, indicating that the signal hypothesis is preferred. The median expectation from a 115 GeV Higgs boson is very close to the observed value.

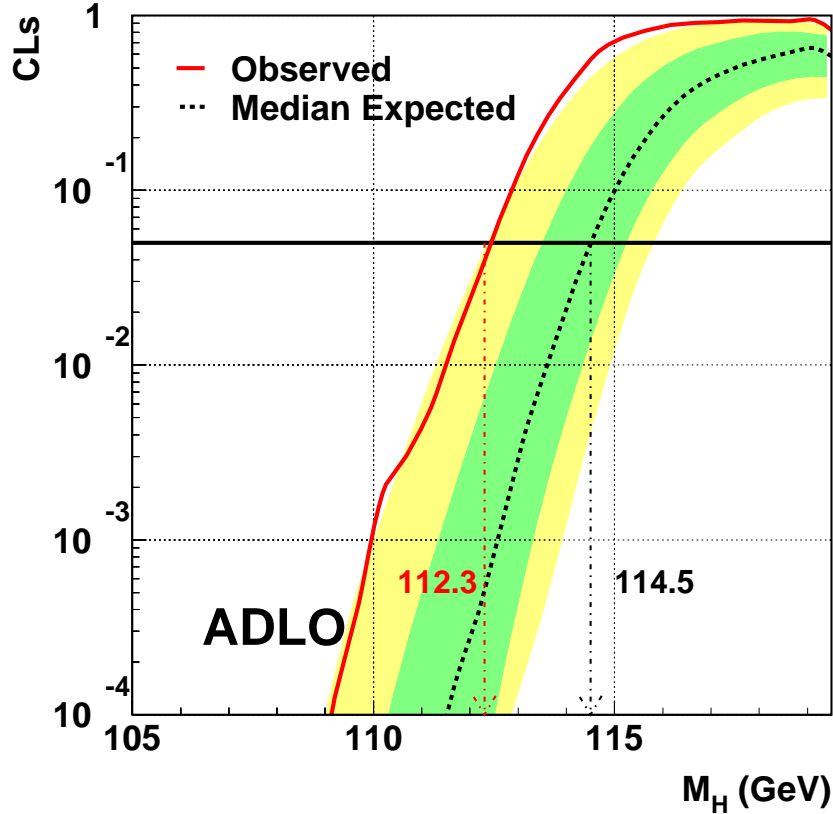


Figure 4: The exclusion confidence level  $CL_s$ , as a function of the test mass  $m_H$ . The solid curve shows the value of  $CL_s$  computed from the selected events observed in the data, for the four LEP experiments combined. The dashed curve is the median expectation in an ensemble of background-only experiments, and the dark and light shaded bands indicate the 68% and 95% probability intervals around the expected median. The 95% CL exclusion limit is the lowest point at which the observed  $CL_s$  crosses 0.05, and the median expected limit is where the median expectation cross the line at 0.05. A lower bound on  $m_H$  is obtained at 112.3 GeV, while the expected limit is 114.5 GeV.

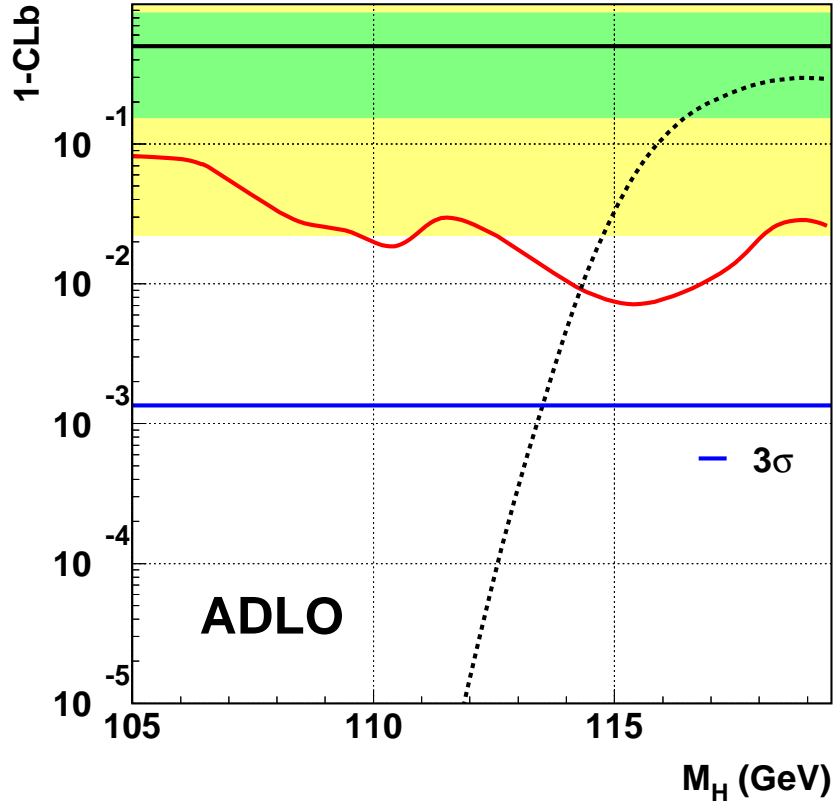


Figure 5: The background confidence level  $1 - CL_b$  as a function of the test mass  $m_H$ . This is the probability of a fluctuation of the background to be at least as signal-like as observed at that particular test mass; a small value indicates an excess of selected events. If  $1 - CL_b < 5.7 \times 10^{-7}$  then a discovery may be claimed at the  $5\sigma$  level. The lowest  $1 - CL_b$  observed in the data is  $7 \times 10^{-3}$  at  $m_H \approx 115$  GeV, which corresponds to a significance of approximately  $2.6\sigma$ .

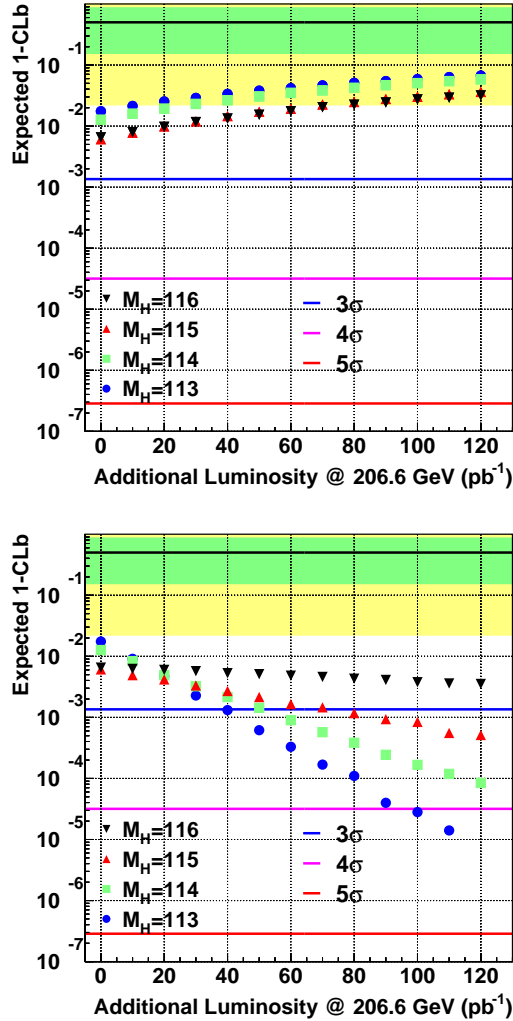


Figure 6: Scenarios for additional LEP running in 2000 beyond the September 5 LEPC. The top pane indicates the expected behavior of  $1 - CL_b$  as a function of the amount of luminosity collected, assuming a beam energy of 206.6 GeV and the absence of a signal, for four different values of the test mass. This quantifies the rapidity with which a background fluctuation should disappear with additional data accumulated. The lower pane indicates the speed with which the significance of an excess will grow with time if the signal were actually present, for different choices of the Higgs boson mass hypothesis  $m_H$ . A 113 GeV Higgs boson would be discoverable with a few months of extra running, but to extend the sensitivity out to 115 GeV requires a run in 2001. LEP typically collects in excess of 1 pb<sup>-1</sup> per day.



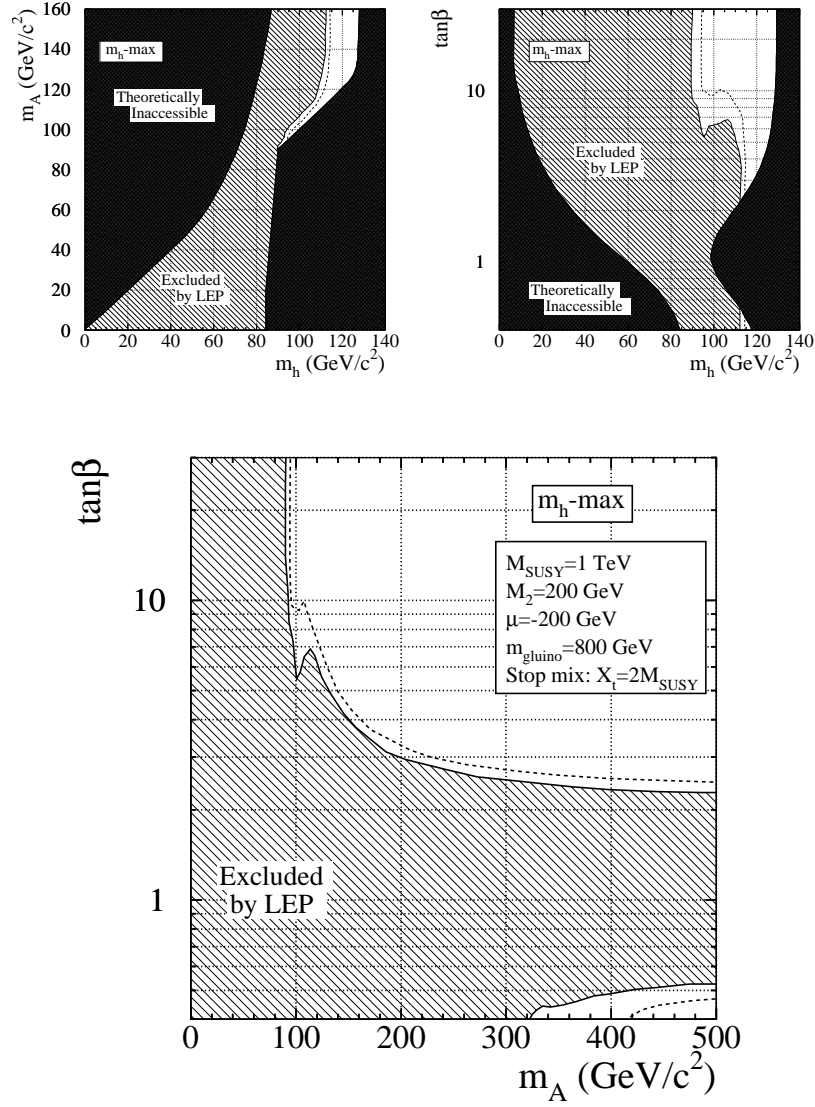


Figure 7: Limits on  $m_h$ ,  $m_A$ , and  $\tan\beta$  in the  $m_h$ -max MSSM benchmark scenario, described in the text. The limits are shown in the  $(m_h, m_A)$  plane (upper left), the  $(m_h, \tan\beta)$  plane (upper right), and in the  $(m_A, \tan\beta)$  plane (lower plot). The excluded regions are shown with diagonal hatching, and the regions which are not allowed by the theory are shown with dark hatching. The median expected boundaries of the excluded regions are shown with dashed lines. The  $m_h$ -max scenario is designed to give the most conservative limits on  $\tan\beta$  from the intersection of the limit curve with the theoretically unallowed region on the right of the  $(m_h, \tan\beta)$  plot.

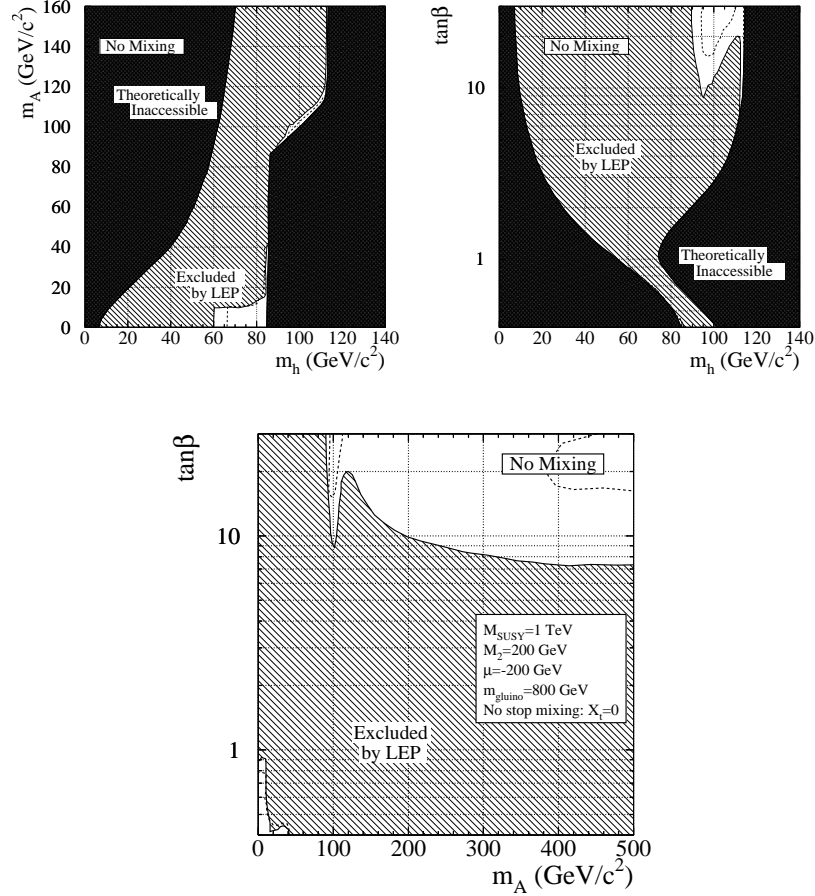


Figure 8: Exclusions in the no-stop-mixing MSSM benchmark scenario, described in the text. The limits are shown in the  $(m_h, m_A)$  plane (upper left), the  $(m_h, \tan\beta)$  plane (upper right), and in the  $(m_A, \tan\beta)$  plane (lower plot). The excluded regions are shown with diagonal hatching, and the regions which are not allowed by the theory are shown with dark hatchings. The median expected boundaries of the excluded regions are shown with dashed lines. In this scenario, the limits are similar for  $m_H \approx m_A$  and also the same for  $m_H$  at low  $\tan\beta$  as they are in the  $m_h$ -max scenario, but the limits on  $\tan\beta$  from the intersection on the right-hand side of the  $(m_h, \tan\beta)$  plot are much more stringent. On the other hand, more parameter space is opened up at low  $\tan\beta$  for values of  $m_h$  between 60 and 85 GeV. In this region, the  $h^0$  decays into  $A^0 A^0$  and/or charm and gluons, because the  $b\bar{b}$  decay is suppressed by the low value of  $\tan\beta$ , and the  $b\bar{b}$  decays of the  $A^0$  are also suppressed. In this region, flavor-independent searches, under development, will be used to search for possible signals, and if none are found, to exclude the remaining part.

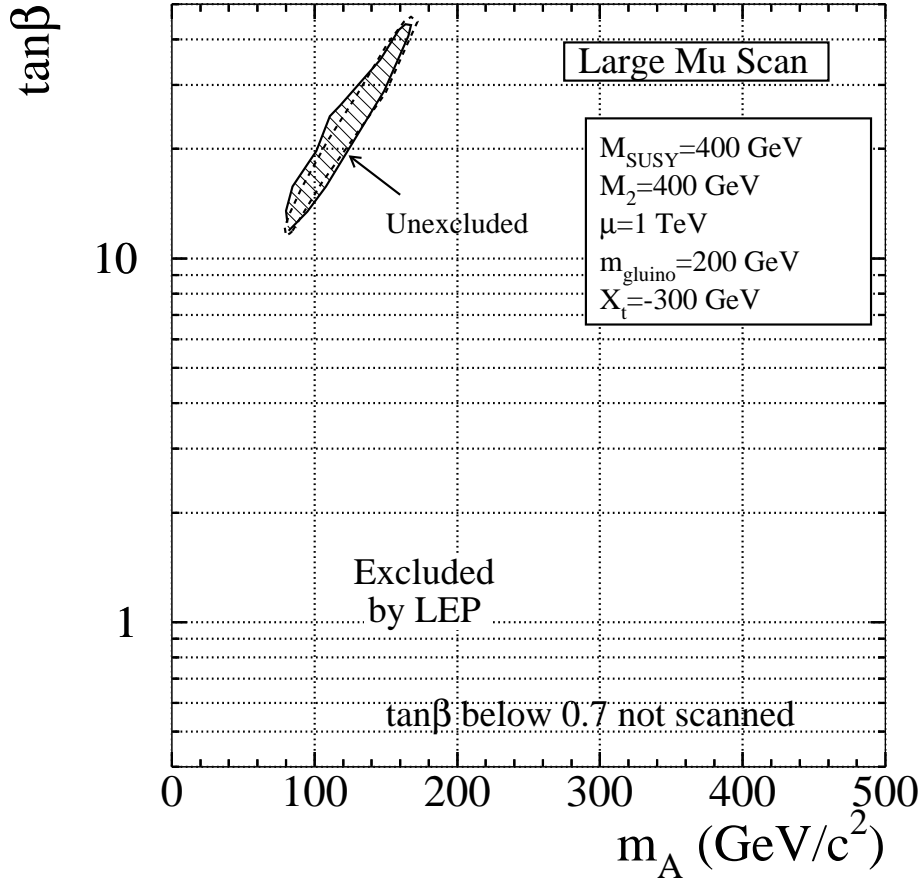


Figure 9: The exclusion in the large- $\mu$  MSSM benchmark scenario, described in the text. Only the  $(m_A, \tan\beta)$  projection is shown because the unexcluded region is not easily visible in the other projections. This scenario is designed to highlight portions of SUSY parameter space where the  $h^0 \rightarrow b\bar{b}$  decay is suppressed, and the tau decays are not enhanced, the remainder being taken up by  $W^{(*)+}W^{(*)-}$  and  $c\bar{c}$  decays. The unexcluded region is shown with diagonal hatching in this case, and the median expected boundary of this region is shown with a dashed line. For some points in this parameter space, the heavy Higgs boson  $H^0$  is kinematically accessible, and the searches for  $h^0 Z^0$  are re-interpreted as searches for  $H^0 Z^0$  where the latter searches have a better expected sensitivity.

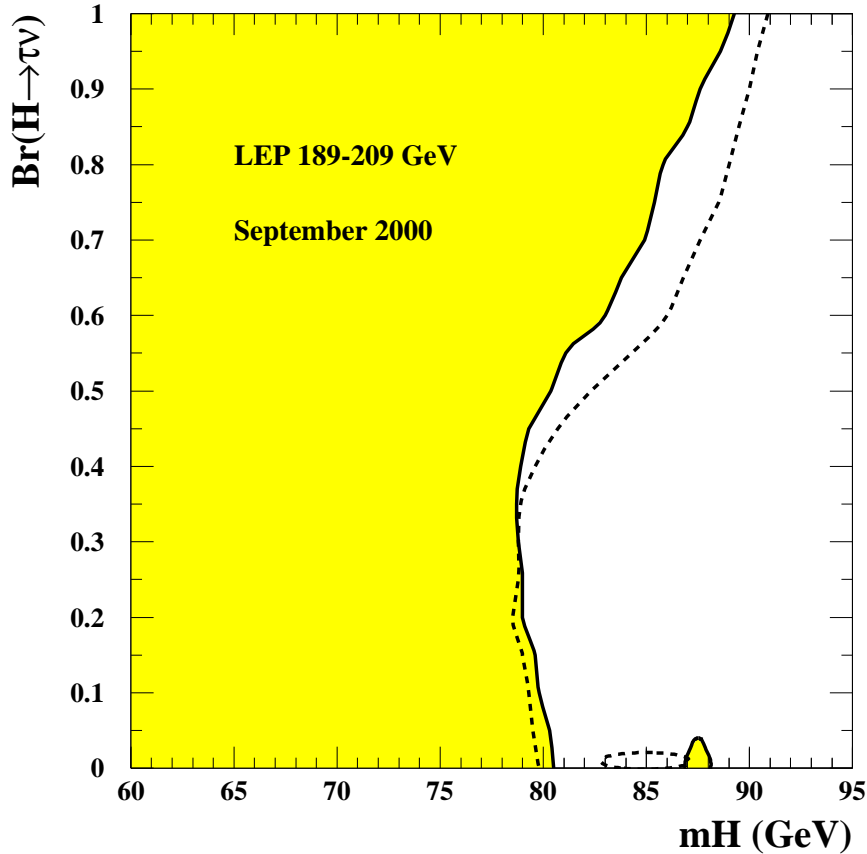


Figure 10: Limits on the production of charged Higgs bosons, as a function of the branching ratio  $\text{Br}(H^+ \rightarrow \tau^+ \nu_\tau)$ , assuming that  $\text{Br}(H^+ \rightarrow \tau^+ \nu_\tau) + \text{Br}(H^+ \rightarrow q\bar{q}') = 1$ . The excluded region is shown with light shading and the boundary is indicated with the heavy solid lines. The boundary of the region expected to be excluded in 50% of background-only experiments is indicated by the dashed lines. The background from  $W^+W^-$  decays is more severe for the four-jet search because of the  $W^\pm$  branching ratios, and impedes efforts to search for charged Higgs bosons with masses close to the mass of the  $W^\pm$ . As data accumulate, though, the sensitivity increase for  $m_{H^\pm}$  significantly in excess of  $m_W$ , and a small island of exclusion is appearing in both the observed and expected limits above  $m_W$  for  $\text{Br}(H^+ \rightarrow \tau^+ \nu_\tau) = 0$ . The result is from the combination of the charged Higgs boson searches from the four LEP experiments.

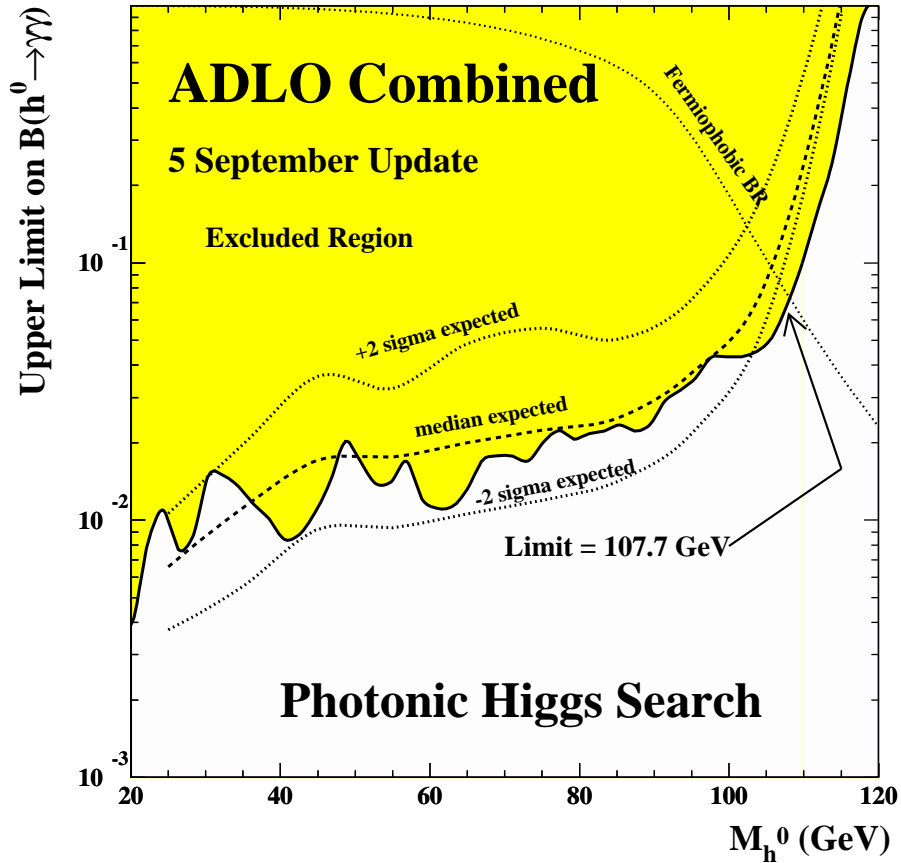


Figure 11: Limits obtained on the production of  $e^+e^- \rightarrow H^0 Z^0 \rightarrow \gamma\gamma Z^0$ , combining all search channels from the four LEP experiments for all decay modes of the  $Z^0$ . These searches are not combined with the searches for the non-photonic decays of the Higgs boson, and are therefore limits on the production cross-section of a Higgs boson which decays only into photons, relative to the Standard Model production cross-section. Alternatively, they are interpreted as limits on the photonic branching ratio of the Higgs boson, ignoring the other search results. A prediction of the photonic branching ratio of the Higgs boson in a model in which the couplings of the Higgs boson to fermions are all zero is shown with the dashed line. In such a fermiophobic model, a lower mass limit of 107.7 GeV is obtained.

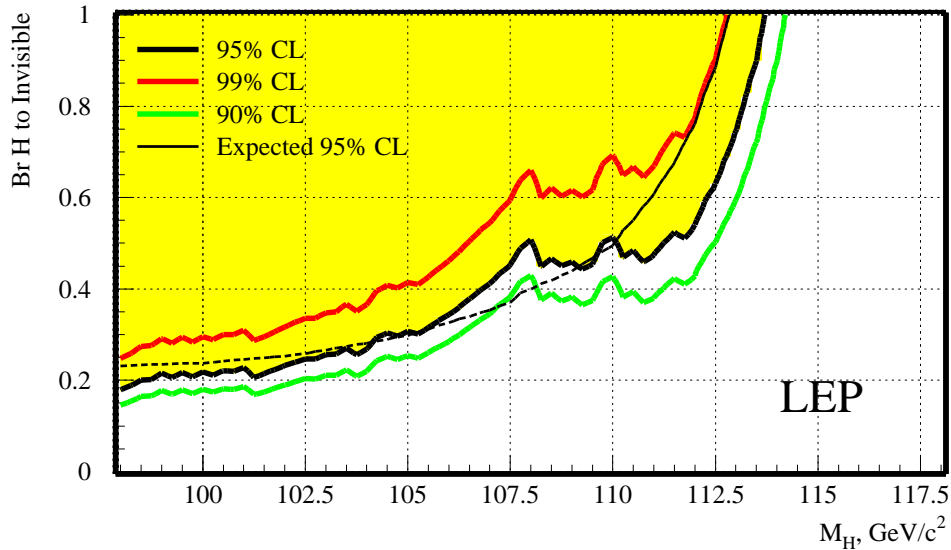


Figure 12: Limits obtained on the production of  $e^+e^- \rightarrow H^0 Z^0$ , where the  $H^0$  decays invisibly, combining all search channels from the four LEP experiments for the included decay modes of the  $Z^0$ . These searches are not combined with the searches for the visible decays of the Higgs boson, and are therefore limits on the production cross-section of a Higgs boson which decays only invisibly, relative to the Standard Model production cross-section. Alternatively, they are interpreted as limits on the invisible branching ratio of the Higgs boson, ignoring the other search results. A lower bound on a Higgs boson produced with the SM production cross-section and decaying invisibly is set at 113.7 GeV, and the median expectation is 112.8 GeV.

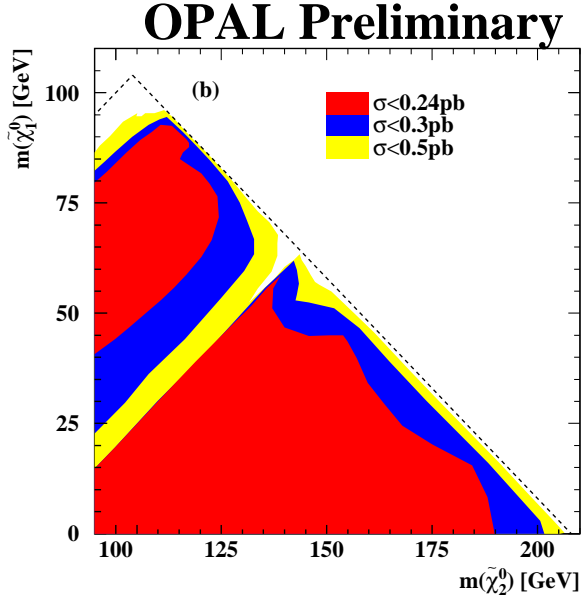
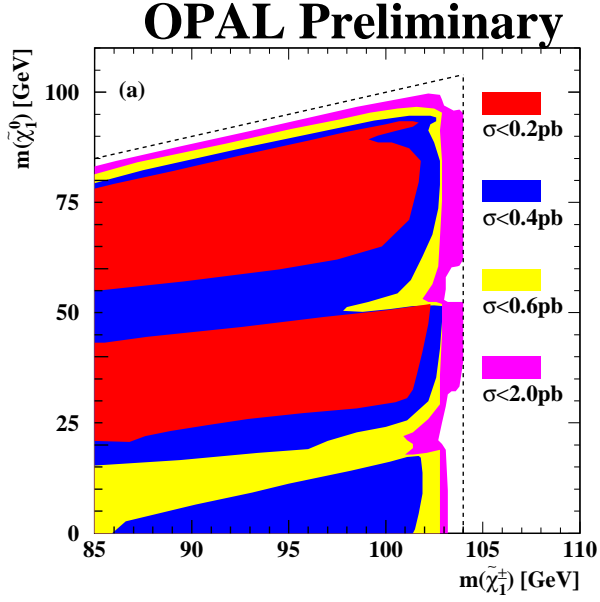


Figure 13: Contours of the 95% C.L. upper limits for (a) the  $e^+e^- \rightarrow \tilde{\chi}_1^+ \tilde{\chi}_1^-$  production cross-sections at  $\sqrt{s} = 208$  GeV are shown assuming  $\text{Br}(\tilde{\chi}_1^+ \rightarrow \tilde{\chi}_1^0 W^{(*)+}) = 100\%$ . (b) the  $e^+e^- \rightarrow \tilde{\chi}_2^0 \tilde{\chi}_1^0$  production cross-sections at  $\sqrt{s} = 208$  GeV are shown assuming  $\text{Br}(\tilde{\chi}_2^0 \rightarrow \tilde{\chi}_1^0 Z^{(*)0}) = 100\%$ . The region for which  $m_{\tilde{\chi}_2^0} + m_{\tilde{\chi}_1^0} < m_Z$  is not considered in this analysis. The limits use only the data taken in 2000.

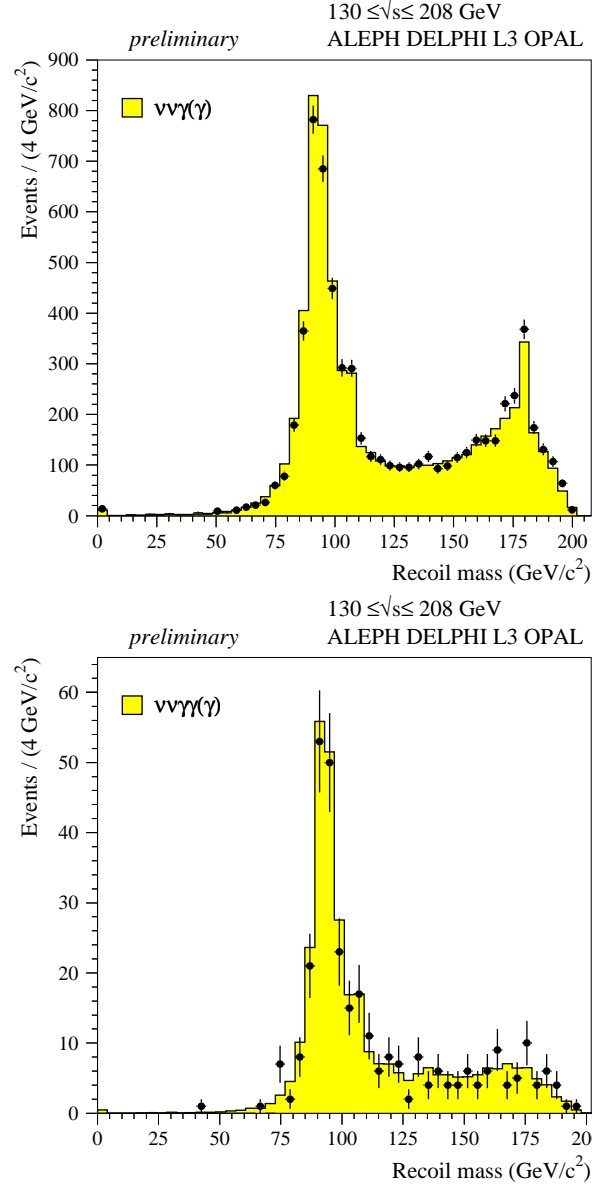


Figure 14: Spectrum of the recoil mass in events with one single high-energy photon (top) and with two or more photons (bottom). Data with  $130 \leq \sqrt{s} \leq 208$  GeV from the four LEP experiments are combined.